[1] **V. S. Loveikin**, D. Sc. (Engineering)
[2] **K. I. Pochka**, Cand. Sc. (Engineering)
[1] **Yu. O. Romasevych**, D. Sc. (Engineering)

[1] National University of Life and Environmental Sciences of Ukraine, Kyiv, Ukraine
e-mail: lovvs@ukr.net
romasevichyuriy@ukr.net
[2] Kyiv National University of Construction and Architecture, Kyiv, Ukraine
e-mail: shanovniy@ukr.net

Keywords: *roll forming unit, drive, force, moment, rigidity, dissipation.*

UDC 693.546

ROLLER FORMING UNIT DYNAMIC ANALYSIS WITH ENERGY BALANCED DRIVE DISSIPATIVE PROPERTIES TAKEN INTO ACCOUNT

In order to increase the reliability and durability of a roller forming unit with an energy-balanced drive, loads in its structure elements and drive are calculated, the function of changing the required moment for ensuring the process of compacting products from building mixtures is determined, taking into account drive dissipation. Dependence of the drive clutch torque on the dissipation coefficient value is established. The recommended values of rigidity and dissipation coefficient for a roller forming unit with an energy-balanced drive are determined.

Problem formulation

During the operation of roller forming units designed for forming reinforced concrete products, considerable dynamic loads appear both in drive and forming trolley elements [1–14]. Despite a rather extensive research into the technological process of forming reinforced concrete products by the non-vibration roller forming method [1–4], the dynamics of a forming trolley movement and its influence on the formation process have not been investigated yet. Little attention has been paid to the modes of a forming trolley movement and the forces arising in drive elements.

Analysis of recent research and publications

In the existing theoretical and experimental studies of roller forming units designed for forming reinforced concrete products, the design parameters and productivity of the units are substantiated [1–4]. At the same time, insufficient attention is paid to the study of the existing dynamic loads and movement modes, which greatly affect both the operation of the units and the quality of the finished products. During continuous start-stop modes, considerable dynamic loads appear both in the drive and forming trolley elements, which may lead to the premature failure of the units [1–6]. Therefore, the task of studying dynamic loads in the elements of the units is actual. In [15–19], loads in the roll forming unit elements were determined, however, the rigidity and dissipation coefficients of the drive were not taken into account.

Purpose of the paper

The purpose of this paper is to determine the loads in the elements of a roll forming unit with an energy-balanced drive, taking into account the drive rigidity and dissipation coefficient.

Statement of the research problem

In order to reduce energy consumption in roller forming machines, a design of a roller forming unit [20, 21] was proposed to provide the compaction of reinforced concrete products on a single technological line. It consists of three forming trolleys, located parallel to each other on one side of the drive shaft, which are set in reciprocating movement from one drive. It is composed of three slider-crank mechanisms, whose cranks are tightly fixed on one drive shaft and shifted to each other at the angle $\Delta\varphi = 120^0$. Fig. 1 shows a roller forming unit with an energy-balanced drive. Each of the forming trolleys 11, 8 and 15 (Fig. 1, a) is mounted on the gantry 14 and performs reciprocating movement in the guide rails 9 over the cavity of the form 10. The forming trolley 11 consists of the feeding hopper 12 and coaxial sections of the compaction rollers 13. The other two trolleys have the same design. The trolleys 11, 8, and 15 with distribution hoppers are set into reciprocating movement by a drive made in the form of three slider-crank mechanisms, whose cranks 5, 3, and 2 are rigidly fixed on one drive shaft 4 and shifted to each other at the angle $\Delta\varphi = 120^0$. The connecting rods 7, 6 and, 1 are hinged to the forming trolleys 11, 8, and 15 while their other ends are

connected to the cranks 5, 3, and 2. Such a design of a roller forming unit makes it possible to reduce the dynamic loads in the drive elements, extra devastating loads on the frame structure and, accordingly, increase the unit durability as a whole. Fig. 1, b shows a kinematic scheme of a roller forming unit with an energy-balanced drive for compacting reinforced concrete products on a single technological line. In this kinematic scheme, r is the radius of the cranks 5, 3, and 2; l is the length of the connecting rods 7, 6, and 1; φ is the angular coordinate of the first trolley crank position; $\Delta\varphi$ is the displacement angle of the cranks 5 and 3, 3 and 2, and 2 and 5 with respect to each other; x_{B_1}, x_{B_2}, and x_{B_3} are the coordinates of the mass centers of the trolleys 11, 8, and 15 respectively; β_1, β_2, and β_3 are the angular coordinates determining the positions of the connecting rods 7, 6 and 1 relative to the horizontal.

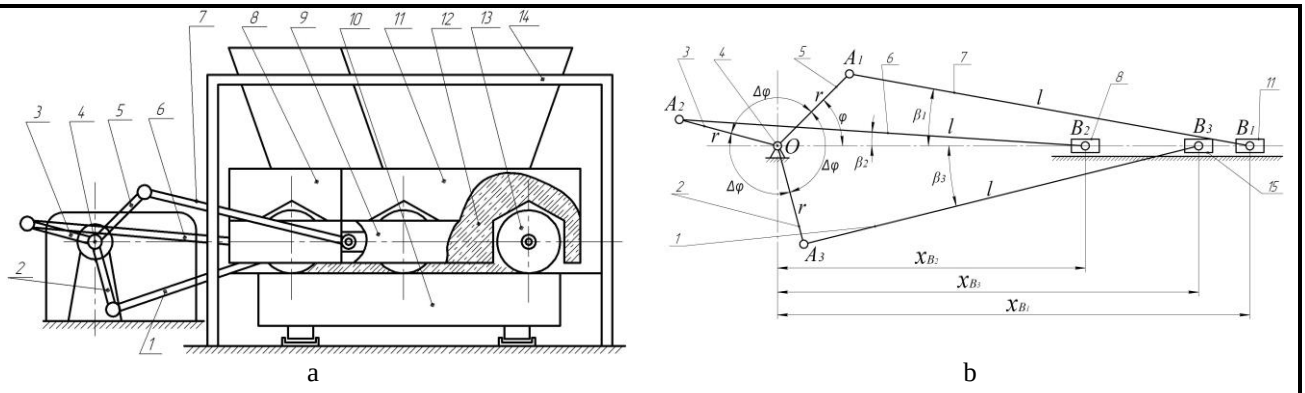

a b

Fig. 1. Roller forming unit with an energy-balanced drive:
a – general view; b – kinematic scheme

During the operation of a roller forming unit with an energy-balanced drive, there arise significant dynamic loads in the elements of the transfer mechanism from the electric motor to the cranks, leading to the premature destruction of the drive structural elements. To study these loads, we use a two-mass dynamic model of a roller forming unit (Fig. 2). In this model, the following symbols are used: M_{dr1} is the driving moment on the driving electric motor shaft, reduced to the crank rotation axis; M_{dr2} is the moment from the movement resistant forces of the forming trolleys with compaction rollers, reduced to the crank rotation axis; J_{dr1} is the inertia moment of the electric motor rotor and drive elements, reduced to the crank rotation axis; J_{dr2} is the inertia moment of the forming trolleys and crank-and-rod mechanisms, reduced to the crank rotation axis; c is the drive mechanism rigidity, reduced to the crank rotation axis; φ_1 and φ_2 are the generalized coordinates of the reduced masses J_{dr1} and J_{dr2}, respectively.

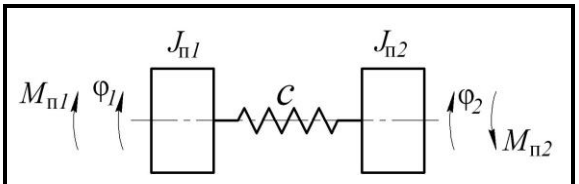

Fig. 2. Dynamic model of a roller forming unit

The drive mechanism reduced moment of inertia can be determined by the following dependence:

$$J_{dr1} = \left(J_{rtr} + J_{cth}\right) \cdot \delta \cdot \mathrm{u}^2, \tag{1}$$

where J_{rtr} and J_{cth} are the moments of inertia of the engine and clutch, connecting the motor shaft and the reducer input shaft, respectively; δ is the coefficient taking into account the moments of inertia of the reducer elements, reduced to the rotor shaft; u is the reducer transmission ratio.

The reduced moment of inertia J_{dr2} can be determined from the second part of the mechanism (Fig. 3), which includes crank-and-rod mechanisms with forming trolleys. In this case, we divide the mass of the connecting rods 7, 6, and 1 m_{conrod} in equal parts in the points A_1 and B_1, A_2 and B_2, and A_3 and B_3. Then the moment of inertia of the cranks can be determined by the dependence

$$J_{crank} = 3 \cdot J'_{crank} + 3 \cdot \frac{m_{conrod}}{2} \cdot r^2 = 3 \cdot \left(J'_{crank} + \frac{m_{conrod}}{2} \cdot r^2 \right), \tag{2}$$

and the trolley masses will have the look

$$m_{B_1} = m'_{B_1} + \frac{m_{conrod}}{2}; \quad m_{B_2} = m'_{B_2} + \frac{m_{conrod}}{2}; \quad m_{B_3} = m'_{B_3} + \frac{m_{conrod}}{2}. \tag{3}$$

In the expressions (3) m_{conrod} is the mass of each of the connecting rods; m'_{B_1}, m'_{B_2}, m'_{B_3} are the masses of the forming trolleys 11, 8 and 15, respectively (Fig. 1, b); J'_{crank} is the moment of inertia of each of the cranks relative to their own rotation axes; r is the radius of each of the cranks; J_{crank} is the moment of inertia of each of the cranks with half the mass of the connecting rod relative to their own rotation axes; m_{B_1}, m_{B_2}, m_{B_3} are the masses of the trolleys 11, 8, and 15 with half the mass of the connecting rod.

The reduced moment of inertia J_{dr2} can be determined from the condition of equality of the kinetic energies of the crank-and-rod mechanisms with the trolleys T_r (Fig. 3) and the second disk of the dynamic model (Fig. 2) T_m, ie. $T_r = T_m$.

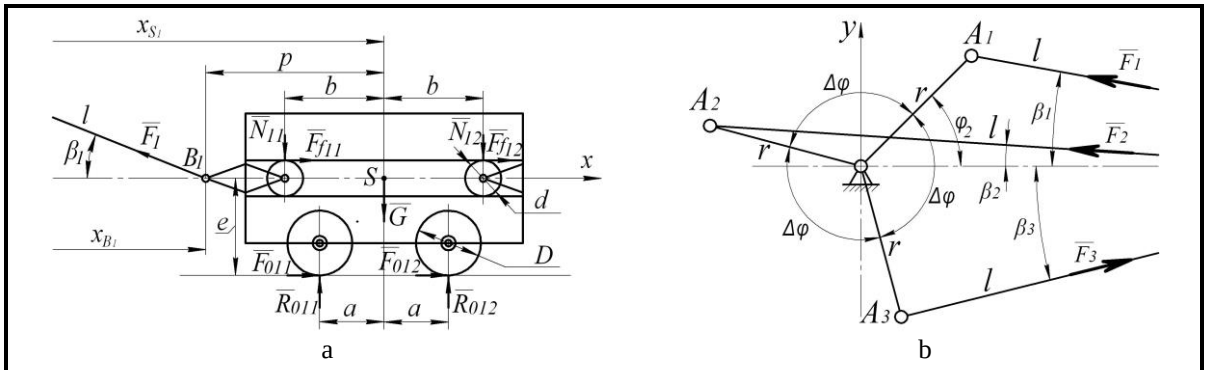

Fig. 3. Calculation scheme of the loads on the elements of a roller forming unit with an energy-balanced drive: a – load on the forming trolley; b – load on the drive mechanism

We find the kinetic energy of crank-and-rod mechanisms with trolleys

$$T_r = \frac{1}{2} \cdot J_{crank} \cdot \dot{\varphi}_2^2 + \frac{1}{2} \cdot m_{B_1} \cdot \dot{x}_{S_1}^2 + \frac{1}{2} \cdot m_{B_2} \cdot \dot{x}_{S_2}^2 + \frac{1}{2} \cdot m_{B_3} \cdot \dot{x}_{S_3}^2, \tag{4}$$

where $\dot{x}_{S_1}$, $\dot{x}_{S_2}$, and $\dot{x}_{S_3}$ are the velocities of the mass centers of the first, second and third forming trolleys, respectively.

Since the three trolleys move progressively, all their points have the same velocity. Therefore, we can accept that $\dot{x}_{S_1} = \dot{x}_{B_1}$, $\dot{x}_{S_2} = \dot{x}_{B_2}$, and $\dot{x}_{S_3} = \dot{x}_{B_3}$. We express the velocities of the points B_1, B_2 та B_3 through the coordinates of the cranks and their derivatives in time. In order to do this, we use the dependencies

$$\dot{x}_{B_1} = \dot{\varphi}_2 \cdot \frac{\partial x_{B_1}}{\partial \varphi_2}; \quad \dot{x}_{B_2} = \dot{\varphi}_2 \cdot \frac{\partial x_{B_2}}{\partial \varphi_2}; \quad \dot{x}_{B_3} = \dot{\varphi}_2 \cdot \frac{\partial x_{B_3}}{\partial \varphi_2}. \tag{5}$$

Then, taking into account (5), the dependence (4) will have the form

$$T_r = \frac{1}{2} \cdot \dot{\varphi}_2^2 \cdot \left[J_{crank} + m_{B_1} \cdot \left(\frac{\partial x_{B_1}}{\partial \varphi_2} \right)^2 + m_{B_2} \cdot \left(\frac{\partial x_{B_2}}{\partial \varphi_2} \right)^2 + m_{B_3} \cdot \left(\frac{\partial x_{B_3}}{\partial \varphi_2} \right)^2 \right]. \tag{6}$$

The kinetic energy of the second disk in figure 2 is expressed by the dependence

$$T_m = \frac{1}{2} \cdot J_{dr2} \cdot \dot{\varphi}_2^2. \tag{7}$$

Equating the dependences (6) and (7), we have

$$\frac{1}{2} \cdot \dot{\varphi}_2^2 \cdot \left[J_{crank} + m_{B_1} \cdot \left(\frac{\partial x_{B_1}}{\partial \varphi_2} \right)^2 + m_{B_2} \cdot \left(\frac{\partial x_{B_2}}{\partial \varphi_2} \right)^2 + m_{B_3} \cdot \left(\frac{\partial x_{B_3}}{\partial \varphi_2} \right)^2 \right] = \frac{1}{2} \cdot J_{dr2} \cdot \dot{\varphi}_2^2. \tag{8}$$

From the equation (8) we obtain

$$J_{dr2} = J_{crank} + m_{B_1} \cdot \left(\frac{\partial x_{B_1}}{\partial \varphi_2} \right)^2 + m_{B_2} \cdot \left(\frac{\partial x_{B_2}}{\partial \varphi_2} \right)^2 + m_{B_3} \cdot \left(\frac{\partial x_{B_3}}{\partial \varphi_2} \right)^2 . \quad (9)$$

To determine the reduced moment of the resistance forces M_{dr2} we use figure 3, on which the following symbols are used: F_1, F_2, and F_3 are the forces in the connecting rods necessary for overcoming the resistance forces acting on the trolleys; β_1, β_2, and β_3 are the angular coordinates determining the positions of the connecting rods of the first, second and third trolleys relative to the horizontal; F_{011} and F_{012} are the horizontal forces of interaction of the compaction rollers with a concrete mixture for the first forming trolley; R_{011} and R_{012} are the vertical forces of interaction of the compaction rollers with a concrete mixture; N_{11} and N_{12} are the normal reactions of the forming trolley guide rails to the guide rollers; $F_{f11} = N_{11} \cdot f_{red}$, $F_{f12} = N_{12} \cdot f_{red}$ are the friction forces of the guide rollers by the forming trolley guide rails; f_{red} is the reduced friction coefficient of the guide rollers by the forming trolley guide rails; G is the forming trolley gravity force; a, b, p, e are the geometric dimensions of the forming trolley; D is the pressure roller diameter; d is the guide roller diameter; l is the connecting rod length. For the second and third forming trolleys, the force parameters F_{021}, F_{022}, F_{031}, F_{032}, R_{021}, R_{022}, R_{031}, R_{032}, N_{21}, N_{22}, N_{31}, N_{32}, F_{f21}, F_{f22}, F_{f31}, F_{f32}, f_{red}, G and the geometric characteristics a, b, p, e, D, d, l will be identical.

To determine the reactions of the guide rollers N_{11}, N_{12}, N_{21}, N_{22}, N_{31}, and N_{32} as well as the forces in the connecting rods F_1, F_2, and F_3, let us consider the static equilibrium of the first, second and third forming trolleys. We design all the forces acting on each of the trolleys on the coordinate axes x and y, and compute the sum of the moments of these forces relative to the points, B_1, B_2, and B_3 (Fig. 3). As a result, for the first forming trolley we obtain

$$\begin{cases} \sum X = -F_1 \cdot \cos\beta_1 + N_{11} \cdot f_{red} + N_{12} \cdot f_{red} + F_{011} + F_{012} = 0; \\ \sum Y = F_1 \cdot \sin\beta_1 - N_{11} - N_{12} - G + R_{011} + R_{012} = 0; \\ \sum M_{B_1} = -N_{11} \cdot (p - b) - N_{12} \cdot (p + b) - G \cdot p - (N_{11} + N_{12}) \cdot f_{red} \cdot \dfrac{d}{2} + \\ \qquad + (F_{011} + F_{012}) \cdot e + R_{011} \cdot (p - a) + R_{012} \cdot (p + a) = 0; \end{cases} \quad (10)$$

for the second forming trolley we obtain

$$\begin{cases} \sum X = -F_2 \cdot \cos\beta_2 + N_{21} \cdot f_{red} + N_{22} \cdot f_{red} + F_{021} + F_{022} = 0; \\ \sum Y = F_2 \cdot \sin\beta_2 - N_{21} - N_{22} - G + R_{021} + R_{022} = 0; \\ \sum M_{B_2} = -N_{21} \cdot (p - b) - N_{22} \cdot (p + b) - G \cdot p - (N_{21} + N_{22}) \cdot f_{red} \cdot \dfrac{d}{2} + \\ \qquad + (F_{021} + F_{022}) \cdot e + R_{021} \cdot (p - a) + R_{022} \cdot (p + a) = 0; \end{cases} \quad (11)$$

for the third forming trolley we obtain

$$\begin{cases} \sum X = -F_3 \cdot \cos\beta_3 + N_{31} \cdot f_{red} + N_{32} \cdot f_{red} + F_{031} + F_{032} = 0; \\ \sum Y = F_3 \cdot \sin\beta_3 - N_{31} - N_{32} - G + R_{031} + R_{032} = 0; \\ \sum M_{B_3} = -N_{31} \cdot (p - b) - N_{32} \cdot (p + b) - G \cdot p - (N_{31} + N_{32}) \cdot f_{red} \cdot \dfrac{d}{2} + \\ \qquad + (F_{031} + F_{032}) \cdot e + R_{031} \cdot (p - a) + R_{032} \cdot (p + a) = 0. \end{cases} \quad (12)$$

Having solved the systems of equations (10) – (12), we find

$$F_1 = \frac{1}{\cos\beta_1 - f_{red}\cdot\sin\beta_1}\cdot\left[\left(R_{011}+R_{012}-G\right)\cdot f_{red}+F_{011}+F_{012}\right]; \tag{13}$$

$$F_2 = \frac{1}{\cos\beta_2 - f_{red}\cdot\sin\beta_2}\cdot\left[\left(R_{021}+R_{022}-G\right)\cdot f_{red}+F_{021}+F_{022}\right]; \tag{14}$$

$$F_3 = \frac{1}{\cos\beta_3 - f_{red}\cdot\sin\beta_3}\cdot\left[\left(R_{031}+R_{032}-G\right)\cdot f_{red}+F_{031}+F_{032}\right]; \tag{15}$$

$$N_{12} = \frac{1}{2\cdot \mathrm{b}}\cdot\left[\begin{array}{l} R_{011}\cdot\left(b-a-f_{red}\cdot\dfrac{d}{2}\right)+R_{012}\cdot\left(b+a-f_{red}\cdot\dfrac{d}{2}\right)- \\ -G\cdot\left(b-f_{red}\cdot\dfrac{d}{2}\right)+F_1\cdot\sin\beta_1\cdot\left(b-p-f_{red}\cdot\dfrac{d}{2}\right)\end{array}\right]; \tag{16}$$

$$N_{22} = \frac{1}{2\cdot \mathrm{b}}\cdot\left[\begin{array}{l} R_{021}\cdot\left(b-a-f_{red}\cdot\dfrac{d}{2}\right)+R_{022}\cdot\left(b+a-f_{red}\cdot\dfrac{d}{2}\right)- \\ -G\cdot\left(b-f_{red}\cdot\dfrac{d}{2}\right)+F_2\cdot\sin\beta_2\cdot\left(b-p-f_{red}\cdot\dfrac{d}{2}\right)\end{array}\right]; \tag{17}$$

$$N_{32} = \frac{1}{2\cdot \mathrm{b}}\cdot\left[\begin{array}{l} R_{031}\cdot\left(b-a-f_{red}\cdot\dfrac{d}{2}\right)+R_{032}\cdot\left(b+a-f_{red}\cdot\dfrac{d}{2}\right)- \\ -G\cdot\left(b-f_{red}\cdot\dfrac{d}{2}\right)+F_3\cdot\sin\beta_3\cdot\left(b-p-f_{red}\cdot\dfrac{d}{2}\right)\end{array}\right]; \tag{18}$$

$$N_{11} = R_{011}+R_{012}+F_1\cdot\sin\beta_1 - N_{12} - G; \tag{19}$$

$$N_{21} = R_{021}+R_{022}+F_2\cdot\sin\beta_2 - N_{22} - G; \tag{20}$$

$$N_{31} = R_{031}+R_{032}+F_3\cdot\sin\beta_3 - N_{32} - G. \tag{21}$$

On the basis of the dependences (13)–(15) we find the moments of the resistance forces M_{res1}, M_{res2} and M_{res3} from each of the forming trolleys and the total moment of the resistance forces M_{dr2}, reduced to the crank rotation axis

$$M_{res1} = F_1\cdot r\cdot\cos\left(\frac{\pi}{2}-\varphi_2-\beta_1\right) = F_1\cdot r\cdot\sin\left(\varphi_2+\beta_1\right); \tag{22}$$

$$M_{res2} = F_2\cdot r\cdot\cos\left(\frac{\pi}{2}-\left(\varphi_2+\Delta\varphi\right)-\beta_2\right) = F_2\cdot r\cdot\sin\left(\varphi_2+\Delta\varphi+\beta_2\right); \tag{23}$$

$$M_{res3} = F_3\cdot r\cdot\cos\left(\frac{\pi}{2}-\left(\varphi_2+2\Delta\varphi\right)-\beta_3\right) = F_3\cdot r\cdot\sin\left(\varphi_2+2\Delta\varphi+\beta_3\right); \tag{24}$$

$$\begin{gathered} M_{dr2} = M_{res1}+M_{res2}+M_{res3} = \\ = F_1\cdot r\cdot\sin\left(\varphi_2+\beta_1\right)+F_2\cdot r\cdot\sin\left(\varphi_2+\Delta\varphi+\beta_2\right)+F_3\cdot r\cdot\sin\left(\varphi_2+2\Delta\varphi+\beta_3\right). \end{gathered} \tag{25}$$

The magnitude of the angles β_1, β_2, and β_3 can be determined from the ratios

$$\mathrm{r}\cdot\sin\varphi_2 = \mathrm{l}\cdot\sin\beta_1; \quad \mathrm{r}\cdot\sin\left(\varphi_2+\Delta\varphi\right) = \mathrm{l}\cdot\sin\beta_2; \quad \mathrm{r}\cdot\sin\left(\varphi_2+2\Delta\varphi\right) = \mathrm{l}\cdot\sin\beta_3. \tag{26}$$

From here

$$\beta_1 = \arcsin\left(\frac{r}{l}\cdot\sin\varphi_2\right); \quad \beta_2 = \arcsin\left(\frac{r}{l}\cdot\sin\left(\varphi_2+\Delta\varphi\right)\right); \quad \beta_3 = \arcsin\left(\frac{r}{l}\cdot\sin\left(\varphi_2+2\Delta\varphi\right)\right). \tag{27}$$

Using the Lagrange equation of the second kind, we make differential equations of the motion of a roller forming unit with an energy-balanced drive, represented by a two-mass dynamic model

$$\begin{aligned}\frac{\mathrm{d}}{\mathrm{dt}}\frac{\partial T}{\partial \dot{\varphi}_1}-\frac{\partial T}{\partial \varphi_1}&=Q_{\varphi_1}-\frac{\partial \Pi}{\partial \varphi_1};\\ \frac{\mathrm{d}}{\mathrm{dt}}\frac{\partial T}{\partial \dot{\varphi}_2}-\frac{\partial T}{\partial \varphi_2}&=Q_{\varphi_2}-\frac{\partial \Pi}{\partial \varphi_2},\end{aligned} \tag{28}$$

where t is the time; T is the system kinetic energy; Q_{φ_1}, Q_{φ_2} are the generalized forces corresponding to the coordinates φ_1 and φ_2; Π is the system potential energy that has the form

$$\Pi=\frac{1}{2}\cdot c\cdot\left(\varphi_1-\varphi_2\right)^2. \tag{29}$$

The system kinetic energy, taking into account the expression (9), is expressed by the dependence

$$T=\frac{1}{2}\cdot J_{dr1}\cdot\dot{\varphi}_1^2+\frac{1}{2}\cdot\left[J_{crank}+m_{B_1}\cdot\left(\frac{\partial x_{B_1}}{\partial\varphi_2}\right)^2+m_{B_2}\cdot\left(\frac{\partial x_{B_2}}{\partial\varphi_2}\right)^2+m_{B_3}\cdot\left(\frac{\partial x_{B_3}}{\partial\varphi_2}\right)^2\right]\cdot\dot{\varphi}_2^2. \tag{30}$$

The generalized forces have the form

$$Q_{\varphi_1}=M_{dr1};\qquad Q_{\varphi_2}=M_{dr2}, \tag{31}$$

where M_{dr1} is the driving moment on the electric motor drive shaft, reduced to the crank rotation axis, which is determined by the Kloss formula

$$M_{dr1}=\frac{2\cdot M_{crit}\cdot \mathrm{u}\cdot\eta_{dr}}{\dfrac{1-\dot{\varphi}_1\cdot\mathrm{u}\,/\,\omega_0}{s_{crit}}+\dfrac{s_{crit}}{1-\dot{\varphi}_1\cdot\mathrm{u}\,/\,\omega_0}}. \tag{32}$$

Here M_{crit} is the critical (maximum) moment on the electric motor shaft; u is the drive mechanism transmission ratio; η_{dr} is the drive mechanism efficiency coefficient; ω_0 is the synchronous angular speed of the electric motor rotor; s_{crit} is the electric motor critical slip determined by the dependence

$$s_{crit}=s_{nom}\cdot\left(\lambda+\sqrt{\lambda^2-1}\right),$$

where λ is the electric motor maximum ratio (electric motor overload capacity); s_{nom} is the electric motor nominal slip determined as follows:

$$s_{nom}=1-\frac{\omega_{nom}}{\omega_0}.$$

Here ω_{nom} is the nominal angular speed of the driving electric motor rotor. Taking the derivatives of the system kinetic energy expression (30), we obtain

$$\begin{aligned}&\frac{\partial T}{\partial\varphi_1}=0;\qquad \frac{\partial T}{\partial\varphi_2}=\dot{\varphi}_2^2\cdot\left[m_{B_1}\cdot\frac{\partial x_{B_1}}{\partial\varphi_2}\cdot\frac{\partial^2 x_{B_1}}{\partial\varphi_2^2}+m_{B_2}\cdot\frac{\partial x_{B_2}}{\partial\varphi_2}\cdot\frac{\partial^2 x_{B_2}}{\partial\varphi_2^2}+m_{B_3}\cdot\frac{\partial x_{B_3}}{\partial\varphi_2}\cdot\frac{\partial^2 x_{B_3}}{\partial\varphi_2^2}\right];\\ &\frac{\partial T}{\partial\dot{\varphi}_1}=J_{dr1}\cdot\dot{\varphi}_1;\qquad \frac{\partial T}{\partial\dot{\varphi}_2}=\left[J_{crank}+m_{B_1}\cdot\left(\frac{\partial x_{B_1}}{\partial\varphi_2}\right)^2+m_{B_2}\cdot\left(\frac{\partial x_{B_2}}{\partial\varphi_2}\right)^2+m_{B_3}\cdot\left(\frac{\partial x_{B_3}}{\partial\varphi_2}\right)^2\right]\cdot\dot{\varphi}_2;\end{aligned} \tag{33}$$

$$\frac{\mathrm{d}}{\mathrm{dt}}\frac{\partial T}{\partial \dot{\varphi}_1} = J_{dr1}\cdot\ddot{\varphi}_1;\quad \frac{\mathrm{d}}{\mathrm{dt}}\frac{\partial T}{\partial \dot{\varphi}_2} = \left[J_{crank} + m_{B_1}\cdot\left(\frac{\partial x_{B_1}}{\partial \varphi_2}\right)^2 + m_{B_2}\cdot\left(\frac{\partial x_{B_2}}{\partial \varphi_2}\right)^2 + m_{B_3}\cdot\left(\frac{\partial x_{B_3}}{\partial \varphi_2}\right)^2\right]\cdot\ddot{\varphi}_2 +$$

$$+\dot{\varphi}_2^2\cdot\left[m_{B_1}\cdot\frac{\partial x_{B_1}}{\partial \varphi_2}\cdot\frac{\partial^2 x_{B_1}}{\partial \varphi_2^2} + m_{B_2}\cdot\frac{\partial x_{B_2}}{\partial \varphi_2}\cdot\frac{\partial^2 x_{B_2}}{\partial \varphi_2^2} + m_{B_3}\cdot\frac{\partial x_{B_3}}{\partial \varphi_2}\cdot\frac{\partial^2 x_{B_3}}{\partial \varphi_2^2}\right].$$

After substituting the expressions (29), (31)–(33), (13)–(15) and (25) into the system of equations (28) we have

$$\begin{cases} J_{dr1}\cdot\ddot{\varphi}_1 = \dfrac{2\cdot M_{crit}\cdot \mathrm{u}\cdot\eta_{dr}}{\dfrac{1-\dot{\varphi}_1\cdot \mathrm{u}/\omega_0}{s_{crit}} + \dfrac{s_{crit}}{1-\dot{\varphi}_1\cdot \mathrm{u}/\omega_0}} - c\cdot(\varphi_1-\varphi_2); \\ \left[J_{crank} + m_{B_1}\cdot\left(\dfrac{\partial x_{B_1}}{\partial \varphi_2}\right)^2 + m_{B_2}\cdot\left(\dfrac{\partial x_{B_2}}{\partial \varphi_2}\right)^2 + m_{B_3}\cdot\left(\dfrac{\partial x_{B_3}}{\partial \varphi_2}\right)^2\right]\cdot\ddot{\varphi}_2 + \\ +\dot{\varphi}_2^2\cdot\left[m_{B_1}\cdot\dfrac{\partial x_{B_1}}{\partial \varphi_2}\cdot\dfrac{\partial^2 x_{B_1}}{\partial \varphi_2^2} + m_{B_2}\cdot\dfrac{\partial x_{B_2}}{\partial \varphi_2}\cdot\dfrac{\partial^2 x_{B_2}}{\partial \varphi_2^2} + m_{B_3}\cdot\dfrac{\partial x_{B_3}}{\partial \varphi_2}\cdot\dfrac{\partial^2 x_{B_3}}{\partial \varphi_2^2}\right] = \\ = c\cdot(\varphi_1-\varphi_2) - \dfrac{1}{\cos\beta_1 - f_{red}\cdot\sin\beta_1}\cdot\left[(R_{011}+R_{012}-G)\cdot f_{red} + F_{011} + F_{012}\right]\cdot r\cdot\sin(\varphi_2+\beta_1) - \\ - \dfrac{1}{\cos\beta_2 - f_{red}\cdot\sin\beta_2}\cdot\left[(R_{021}+R_{022}-G)\cdot f_{red} + F_{021} + F_{022}\right]\cdot r\cdot\sin(\varphi_2+\Delta\varphi+\beta_2) - \\ - \dfrac{1}{\cos\beta_3 - f_{red}\cdot\sin\beta_3}\cdot\left[(R_{031}+R_{032}-G)\cdot f_{red} + F_{031} + F_{032}\right]\cdot r\cdot\sin(\varphi_2+2\Delta\varphi+\beta_3). \end{cases} \quad (34)$$

Results of the solution

For a roller forming unit with the parameters [4] to be given below, the functions are determined and the graphs are built, expressing the changes in the reactions of the guide rollers N_{11}, N_{12}, N_{21}, N_{22}, N_{31}, and N_{32} (Fig. 4), forces in the connecting rods F_1, F_2, and F_3 (Fig. 5), and moments of the resistance forces M_{res1}, M_{res2}, M_{res3} and M_{dr2} (Fig. 6), depending on the rotation angle of the cranks. These parameters are the following: $r = 0.2\ m$; $l = 0.8\ m$; horizontal interaction forces $F_{011} = F_{012} = F_{021} = F_{022} = F_{031} = F_{032} = 7962\ N$ between the compaction rollers and a concrete mixture during the process of its being compacted by a roller forming trolley with two $R = 0.11\ m$ compaction rollers, the mixture having the following characteristics: product height $h_0 = 0.22\ m$; product width $B = 1.164\ m$; type of compacted mixture is fine-grained; concrete mixture humidity $W = 10\%$; required product compactness $k_{comp} = 0.98$; value of the maximum contact pressure providing $k_{comp} = 0.98$ at $W = 10\%$, according to experimental data $p = 625\ kPa$; $R_{011} = R_{012} = R_{021} = R_{022} = R_{031} = R_{032} = 9740\ N$; $m_{conrod} = 64\ kg$; $m'_{B_1} = m'_{B_2} = m'_{B_3} = 1000\ kg$; $f_{red} = 0.008$; $D = 0.22\ m$; $\mathrm{d} = 0.046\ m$; $a = 0.27\ m$; $b = 0.37\ m$; $p = 0.52\ m$; $e = 0.21\ m$; trolley mass with half the mass of the connecting rod $m_{B_1} = m_{B_2} = m_{B_3} = 1032\ kg$; $G = 10124.9\ N$ by the expressions (13)-(25), taking into account (27).

The nominal rated power of the electric motor is determined by the mean value of the reduced moment of resistance for one crank rotation cycle [22, 23]. According to these data, a 4A series 4A160M6У3 basic-version asynchronous electric motor with a short-circuit rotor was chosen, having the following parameters: engine rotor synchronous speed $\omega_o = 104.72\ rad/s$; engine rotor nominal speed

$\omega_{nom} = 102.1\ rad/s$; engine rotor critical speed $\omega_{crit} = 94.95\ rad/s$; engine rotor moment of inertia $J_{rtr} = 0.183\ kg \cdot m^2$; starting moment $M_{start} = 176.3\ N \cdot m$; nominal moment $M_{nom} = 146.915\ N \cdot m$; critical moment $M_{crit} = 293.83\ N \cdot m$; overload capacity $\lambda = M_{crit} / M_{nom} = 2.0$; nominal slip $s_{nom} = 0.025$; critical slip $s_{crit} = 0.0933$. In addition, the PF (pin flexible) claw clutch [25] having the nominal transfer torque $M_{nom} = 500\ N \cdot m$ and moment of inertia $J_{cth} = 0.32\ kg \cdot m^2$ as well as the C2-400 reducer [25] with the transmission ratio $u = 9.8$ and moment of inertia $J_{red} = 0.046\ kg \cdot m^2$ were selected.

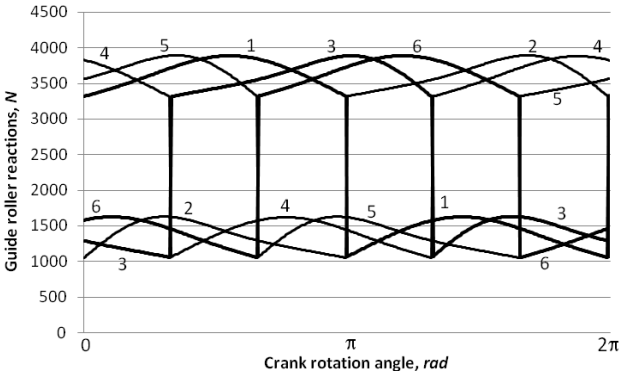

Fig. 4. Charts of the reaction changes of the guide rollers N_{11} (1), N_{12} (2), N_{21} (3), N_{22} (4), N_{31} (5), and N_{32} (6), depending on the rotation angle of the cranks

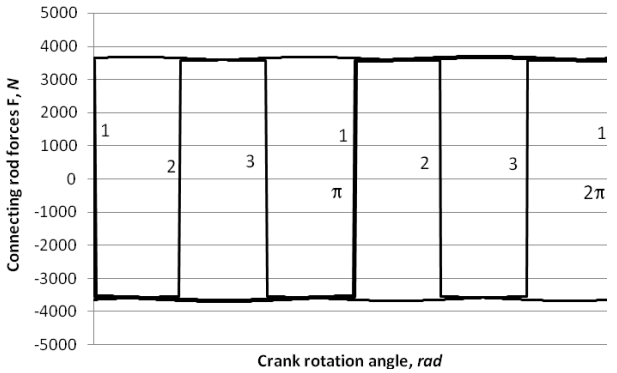

Fig. 5. Chart of the force changes in the connecting rods F_1 (1), F_2 (2), F_3 (3) depending on the rotation angle of the cranks

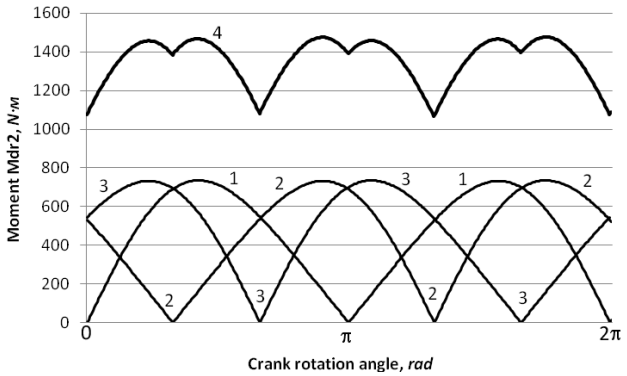

Fig. 6. Chart of the resistance force changes M_{res1} (1), M_{res2} (1), M_{res3} (3) and M_{dr2} (4) depending on the rotation angle of the cranks

The values of the first and second transfer functions of the trolleys are determined from the expressions of the functions of changing the coordinates of the first, second and third forming trolleys in accordance with (Fig. 1, b) [5, 15, 22, 23]

$$x_{B_1} = r \cdot \cos\varphi_2 + l \cdot \cos\beta_1; \tag{35}$$

$$x_{B_2} = r \cdot \cos(\varphi_2 + \Delta\varphi) + l \cdot \cos\beta_2; \tag{36}$$

$$x_{B_3} = r \cdot \cos(\varphi_2 + 2\Delta\varphi) + l \cdot \cos\beta_3. \tag{37}$$

From the equations (26) we can obtain

$$\sin\beta_1 = \frac{r}{l}\cdot\sin\varphi_2 \;\rightarrow\; \cos\beta_1 = \left[1-\left(\frac{r}{l}\cdot\sin\varphi_2\right)^2\right]^{\frac{1}{2}}; \tag{38}$$

$$\sin\beta_2 = \frac{r}{l}\cdot\sin\left(\varphi_2+\Delta\varphi\right) \;\rightarrow\; \cos\beta_2 = \left[1-\left(\frac{r}{l}\cdot\sin\left(\varphi_2+\Delta\varphi\right)\right)^2\right]^{\frac{1}{2}}; \tag{39}$$

$$\sin\beta_3 = \frac{r}{l}\cdot\sin\left(\varphi_2+2\Delta\varphi\right) \;\rightarrow\; \cos\beta_3 = \left[1-\left(\frac{r}{l}\cdot\sin\left(\varphi_2+2\Delta\varphi\right)\right)^2\right]^{\frac{1}{2}}. \tag{40}$$

The expressions $\cos\beta_1$, $\cos\beta_2$, and $\cos\beta_3$ in the expressions (38)–(40), can be expanded into series by Newton's binomial formula

$$\left[1-\left(\frac{r}{l}\cdot\sin\varphi_2\right)^2\right]^{\frac{1}{2}} = 1-\frac{1}{2}\cdot\left(\frac{r}{l}\cdot\sin\varphi_2\right)^2-\frac{1}{8}\cdot\left(\frac{r}{l}\cdot\sin\varphi_2\right)^4-\ldots; \tag{41}$$

$$\left[1-\left(\frac{r}{l}\cdot\sin\left(\varphi_2+\Delta\varphi\right)\right)^2\right]^{\frac{1}{2}} = 1-\frac{1}{2}\cdot\left(\frac{r}{l}\cdot\sin\left(\varphi_2+\Delta\varphi\right)\right)^2-\frac{1}{8}\cdot\left(\frac{r}{l}\cdot\sin\left(\varphi_2+\Delta\varphi\right)\right)^4-\ldots; \tag{42}$$

$$\left[1-\left(\frac{r}{l}\cdot\sin\left(\varphi_2+2\Delta\varphi\right)\right)^2\right]^{\frac{1}{2}} = 1-\frac{1}{2}\cdot\left(\frac{r}{l}\cdot\sin\left(\varphi_2+2\Delta\varphi\right)\right)^2-\frac{1}{8}\cdot\left(\frac{r}{l}\cdot\sin\left(\varphi_2+2\Delta\varphi\right)\right)^4-\ldots. \tag{43}$$

The ratios $\frac{r}{l}$ for roller forming units with crank-and-rod drive mechanisms do not exceed ⅓, and the series (41)–(43) converge fairly quickly, so, with satisfactory for the practice accuracy, the third and subsequent members of the series (41)–(43) can be thrown away. Then the dependencies (35)–(37) will look as

$$x_{B_1} = r\cdot\cos\varphi_2 + l\cdot\left[1-\frac{1}{2}\cdot\left(\frac{r}{l}\cdot\sin\varphi_2\right)^2\right]; \tag{44}$$

$$x_{B_2} = r\cdot\cos\left(\varphi_2+\Delta\varphi\right) + l\cdot\left[1-\frac{1}{2}\cdot\left(\frac{r}{l}\cdot\sin\left(\varphi_2+\Delta\varphi\right)\right)^2\right]; \tag{45}$$

$$x_{B_3} = r\cdot\cos\left(\varphi_2+2\Delta\varphi\right) + l\cdot\left[1-\frac{1}{2}\cdot\left(\frac{r}{l}\cdot\sin\left(\varphi_2+2\Delta\varphi\right)\right)^2\right]. \tag{46}$$

The values of the first and second transfer functions of all three forming trolleys are determined from the expressions (44)–(46) by the following dependencies:

$$\begin{gathered}\frac{\partial x_{B_1}}{\partial\varphi_2} = -r\cdot\left(\sin\varphi_2+\frac{r}{2\cdot l}\cdot\sin 2\varphi_2\right);\quad \frac{\partial x_{B_2}}{\partial\varphi_2} = -r\cdot\left[\sin\left(\varphi_2+\Delta\varphi\right)+\frac{r}{2\cdot l}\cdot\sin 2\left(\varphi_2+\Delta\varphi\right)\right];\\ \frac{\partial x_{B_3}}{\partial\varphi_2} = -r\cdot\left[\sin\left(\varphi_2+2\Delta\varphi\right)+\frac{r}{2\cdot l}\cdot\sin 2\left(\varphi_2+2\Delta\varphi\right)\right];\end{gathered} \tag{47}$$

$$\frac{\partial^2 x_{B_1}}{\partial \varphi_2^2} = -r \cdot \left(\cos\varphi_2 + \frac{r}{l} \cdot \cos 2\varphi_2 \right); \quad \frac{\partial^2 x_{B_2}}{\partial \varphi_2^2} = -r \cdot \left[\cos(\varphi_2 + \Delta\varphi) + \frac{r}{l} \cdot \cos 2(\varphi_2 + \Delta\varphi) \right];$$
$$\frac{\partial^2 x_{B_3}}{\partial \varphi_2^2} = -r \cdot \left[\cos(\varphi_2 + 2\Delta\varphi) + \frac{r}{l} \cdot \cos 2(\varphi_2 + 2\Delta\varphi) \right]. \tag{48}$$

As a result of the numerical experiment, it has been established that the optimal value of the rigidity, reduced to the crank rotation axis, of the drive of a roller forming unit with an energy-balanced drive with the above parameters equals $c = 150000 \ {}^{N}\!/_{m}$. The determination of the optimal value of the drive rigidity was carried out according to the method described in papers [26, 27]. At this rigidity value, minimum loads are observed in the drive clutches. This rigidity value is used in the following calculations.

To study the movement dynamics of a roller forming unit with one taking into account the dissipation during the start-stop movement modes of forming trolleys, the system of equations (34) was supplemented by the drive dissipation value k

$$\begin{cases} J_{dr1} \cdot \ddot{\varphi}_1 = \dfrac{2 \cdot M_{crit} \cdot u \cdot \eta_{dr}}{\dfrac{1 - \dot{\varphi}_1 \cdot u / \omega_0}{s_{crit}} + \dfrac{s_{crit}}{1 - \dot{\varphi}_1 \cdot u / \omega_0}} - c \cdot (\varphi_1 - \varphi_2) - k \cdot (\dot{\varphi}_1 - \dot{\varphi}_2); \\ \left[J_{crank} + m_{B_1} \cdot \left(\dfrac{\partial x_{B_1}}{\partial \varphi_2} \right)^2 + m_{B_2} \cdot \left(\dfrac{\partial x_{B_2}}{\partial \varphi_2} \right)^2 + m_{B_3} \cdot \left(\dfrac{\partial x_{B_3}}{\partial \varphi_2} \right)^2 \right] \cdot \ddot{\varphi}_2 + \\ + \dot{\varphi}_2^2 \cdot \left[m_{B_1} \cdot \dfrac{\partial x_{B_1}}{\partial \varphi_2} \cdot \dfrac{\partial^2 x_{B_1}}{\partial \varphi_2^2} + m_{B_2} \cdot \dfrac{\partial x_{B_2}}{\partial \varphi_2} \cdot \dfrac{\partial^2 x_{B_2}}{\partial \varphi_2^2} + m_{B_3} \cdot \dfrac{\partial x_{B_3}}{\partial \varphi_2} \cdot \dfrac{\partial^2 x_{B_3}}{\partial \varphi_2^2} \right] = \\ = c \cdot (\varphi_1 - \varphi_2) + k \cdot (\dot{\varphi}_1 - \dot{\varphi}_2) - \\ - \dfrac{1}{\cos\beta_1 - f_{red} \cdot \sin\beta_1} \cdot \left[(R_{011} + R_{012} - G) \cdot f_{red} + F_{011} + F_{012} \right] \cdot r \cdot \sin(\varphi_2 + \beta_1) - \\ - \dfrac{1}{\cos\beta_2 - f_{red} \cdot \sin\beta_2} \cdot \left[(R_{021} + R_{022} - G) \cdot f_{red} + F_{021} + F_{022} \right] \cdot r \cdot \sin(\varphi_2 + \Delta\varphi + \beta_2) - \\ - \dfrac{1}{\cos\beta_3 - f_{red} \cdot \sin\beta_3} \cdot \left[(R_{031} + R_{032} - G) \cdot f_{red} + F_{031} + F_{032} \right] \cdot r \cdot \sin(\varphi_2 + 2\Delta\varphi + \beta_3). \end{cases} \tag{49}$$

Having solved the system of equations (49), taking into account the expressions (2), (27), (47) and (48), a graphical dependency of the change of the maximum $M_{cth\,\max}$ (Fig. 7) and the mean square $\tilde{M}_{cth}$ (Fig. 8) torques in the clutch was determined and built, depending on the dissipation coefficient. The analysis of the graphs shows that at all the values of the dissipation coefficient in the range from $k = 100 \ \dfrac{N \cdot \sec}{m}$ up to $k = 15000 \ \dfrac{N \cdot \sec}{m}$ the maximum and the mean square torques decrease, however, a in the range from $k = 100 \ \dfrac{N \cdot \sec}{m}$ up to $k = 8000 \ \dfrac{N \cdot \sec}{m}$ they change sharply, and then stabilize smoothly, which almost does not affect the dynamics of the unit movement.

Proceeding from the system of equations (49), the graphs of the torque change in the clutch M_{cth} (Fig. 9) were calculated and built for the steady movement section, depending on the time at the values of the dissipation coefficient $k = 2000 \ \dfrac{N \cdot \sec}{m}$ (position 1) and dissipation coefficient $k = 10000 \ \dfrac{N \cdot \sec}{m}$ (position 2). The analy-

sis of these graphs shows that when the drive dissipation coefficient $k = 2000\ \frac{N \cdot \sec}{m}$, the torque value in the clutch in the steady movement mode changes in the range from $M_{cth\ \min} = -1450\ N \cdot m$ to $M_{cth\ \max} = 1330\ N \cdot m$. At the drive dissipation coefficient $k = 10000\ \frac{N \cdot \sec}{m}$, the torque value in the clutch in the steady movement mode changes in the range from $M_{cth\ \min} = -600\ N \cdot m$ to $M_{cth\ \max} = 580\ N \cdot m$.

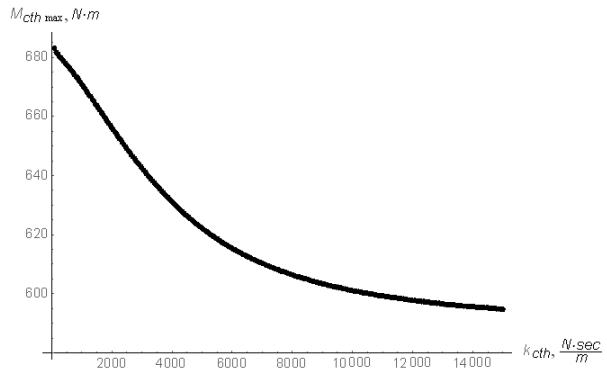

Fig. 7. Chart of the maximum torque $M_{cth\ \max}$ changes in the clutch, depending on the dissipation coefficient

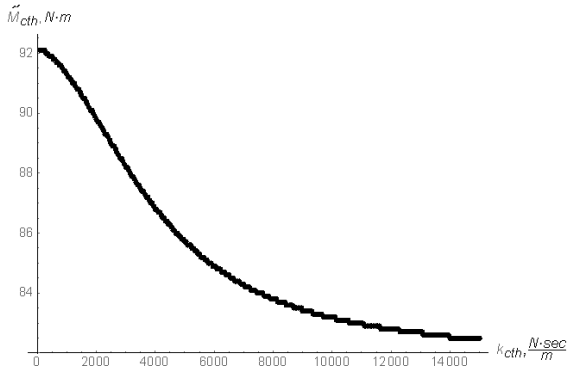

Fig. 8. Chart of the mean square torque $\tilde{M}_{cth}$ change in the clutch, depending on the dissipation coefficient

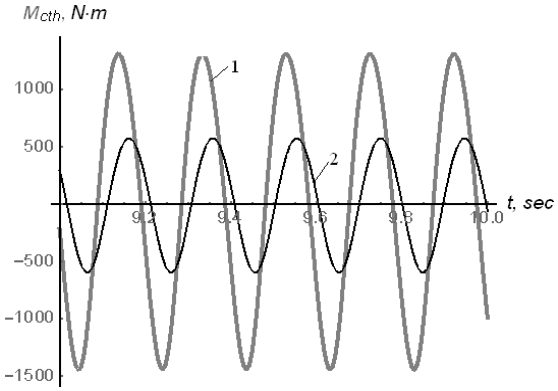

Fig. 9. Chart of the torque in the clutch M_{cth}, depending on the time

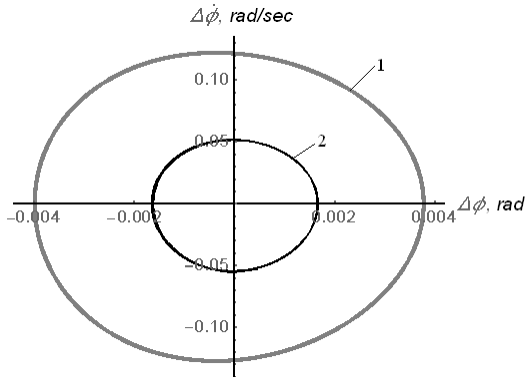

Fig. 10. Graphic dependence $((\varphi_1 - \varphi_2), (\dot{\varphi}_1 - \dot{\varphi}_2))$

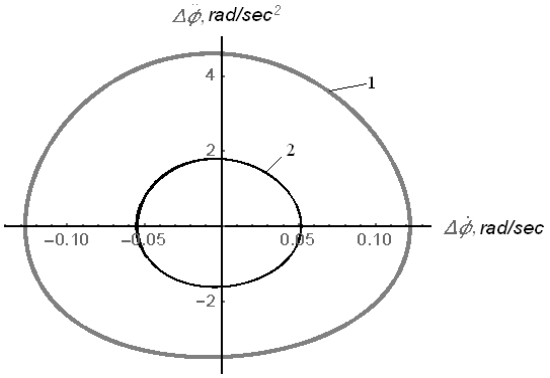

Fig. 11. Graphic dependence $((\dot{\varphi}_1 - \dot{\varphi}_2), (\ddot{\varphi}_1 - \ddot{\varphi}_2))$

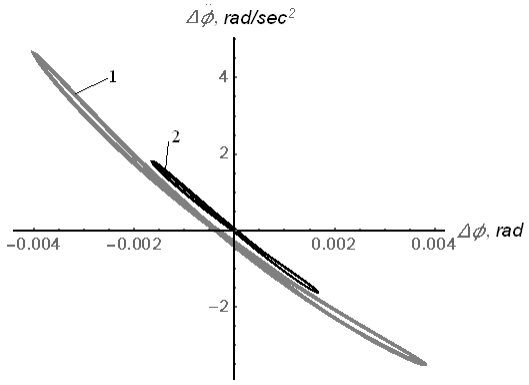

Fig. 12. Graphic dependence $((\dot{\varphi}_1 - \dot{\varphi}_2), (\ddot{\varphi}_1 - \ddot{\varphi}_2))$

Fig. 10–12 show the graphic dependencies $((\varphi_1-\varphi_2),(\dot{\varphi}_1-\dot{\varphi}_2))$, $((\dot{\varphi}_1-\dot{\varphi}_2),(\ddot{\varphi}_1-\ddot{\varphi}_2))$, and $((\varphi_1-\varphi_2),(\ddot{\varphi}_1-\ddot{\varphi}_2))$ at the dissipation coefficient values $k=2000\ \frac{N\cdot\sec}{m}$ (position 1) and $k=10000\ \frac{N\cdot\sec}{m}$ (position 2), respectively. The analysis of these graphs shows the identical nature of their changes, but at the drive dissipation coefficient value $k=2000\ \frac{N\cdot\sec}{m}$ their amplitude along the abscissa and ordinate axes is more important than at $k=10000\ \frac{N\cdot\sec}{m}$.

Conclusions

1. As a result of the research carried out in order to increase the reliability and durability of a roller forming unit with an energy-balanced drive, the loads in both its elements and drive were calculated, and the function of changing the required torque on the crank drive shaft was determined to ensure the compaction of products from building mixtures, taking into account the rigidity and dissipation of the drive.

2. For a roller forming unit with an energy-balanced drive, the drive rigidity value, reduced to the crank rotation axis, is determined, at which the minimum loads are observed in the drive clutches.

3. The dependence of the torque in the drive clutch on the dissipation coefficient values is analyzed.

4. For a roller molding unit with an energy-balanced drive with the above parameters, the recommended value of the dissipation coefficient is in the range from $k=8000\ \frac{N\cdot\sec}{m}$ to $k=10000\ \frac{N\cdot\sec}{m}$. Increasing the dissipation coefficient value will not significantly affect the unit dynamics, but will require more precision in the manufacture of the drive.

5. The results of the work may in the future be useful to refine and improve the existing engineering methods for estimating the drives of roller forming units, both at design stages and in practical use.

References

1. Harnets V. M. Prohresyvni betonoformuiuchi ahrehaty i kompleksy. [Progressive Concrete the Forming Units and Complexes]. Kyiv: Budivelnyk, 1991. 144 p. (in Ukrainian).
2. Harnets V. M., Zaichenko S. V., Chovniuk Yu. V., Shalenko V. O., Prykhodko Ya. S. Concrete the Forming Units. Constructive and Functional to the Scheme, Principle of Action, Theory Basis]. Kyiv: Interservis, 2015. 238 p. (in Ukrainian).
3. Kuzin V. N. Technology of Roller Formation of Flat Articles from Fine-Grained Concrete: Extended abstract of candidate thesis / Moscow construction instituteю Moscow, USSR. 1981 (in Russian).
4. Ryushin V. T. Issledovanie rabochego protsessa i razrabotka metodiki rascheta mashin rolikovogo formovaniya betonnykh smesey [Research of Working Process and Development of a Method of Calculation of Machines of Roller Formation of Concrete Mixes]: Unpublished candidate thesis / Kyiv construction institute. Kyiv, USSR. 1986 (in Russian).
5. Loveikin V. S. & Pochka K. I. Dynamichnyi analiz rolykovoi formovochnoi ustanovky z rekuperatsiinym pryvodom. [The Dynamic Analysis of Roller Forming Installation with the Recuperative Drive]. *Dynamics, durability and reliability of farm vehicles*: Works of the first Intern. sci. and techn. conf. (DSR AM-I). (Ternopil, October 2004) Ternopil, 2004. P. 507–514 (in Ukrainian).
6. Loveikin V. S. & Pochka K. I. Rezultaty eksperymentalnykh doslidzhen rezhymiv rukhu rolykovoi formuvalnoi ustanovky z rekuperatsiinym pryvodom. [Results of Pilot Studies of the Modes of the Movement of Roller Forming Installation with the Recuperative drive]. *The bulletin of the Kharkov nat. university of agriculture of P. Vasilenko.* 2007. Vol. 1. No. 59. P. 465–474 (in Ukrainian).
7. Nazarenko I. I., Smirnov V. M., Pelevin L. Ye., Fomin A. V., Sviderskyi A. T., Kosteniuk O. O., Ruchynskyi M. M., Diedov O. P., Harkavenko O. M., Martyniuk I. Yu. Osnovy teorii rukhu zemleryinykh i ushchilniuvalnykh mashyn budindustrii z kerovanymy u chasi optymalnymy parametramy [Fundamentals of the Theory of the Movement of the Digging and Condensing Machines of the Construction Industry with the Optimum Parameters Operated in Time]. Kyiv: MP Lesia, 2013. 188 p. (in Ukrainian).
8. Zaichenko S., Shalenko V., Shevchuk N. & Vapnichna V. Development of a Geomechanic Complex for Geotechnical Monitoring Contour Mine Groove. *Eastern-European Journal of Enterprise Technologies*. 2017. Vol. 3/9 (87). P. 19–25. DOI: 10.155/1729-4061.2017.102067.

9. Harnets V. M., Chovniuk Yu. V., Zaichenko S. V., Shalenko V. O., Prykhodko Ya. S. Teoriia i praktyka stvorennia betonoformuvalnykh ahrehativ [Theory and Practice of Creation of Units of Formation of Concrete]. *Mining, construction, road and meliorative machines.* 2014. No. 83. P. 49–54 (in Ukrainian).
10. Harnets V. M., Zaichenko S. V., Prykhodko Ya. S., Shalenko V. O. Rozrobka naukovo-praktychnykh rekomendatsii po stvorenniu betonoformuiuchykh ahrehativ (BFA). [Development of Scientific and Practical Recommendations About Creation of Units of Formation of Concrete]. *Mining, construction, road and meliorative machines*. 2012. No. 79. P. 46–52 (in Ukrainian).
11. Zaichenko S. V., Shevchuk S. P., Harnets V. M. Enerhetychnyi analiz protsesu rolykovoho ushchilnennia. Enerhetyka: Ekonomika, tekhnolohiia, ekolohiia. [Power Analysis of Process of Roller Consolidation]. *Power: Economy, technology, ecology*. 2012. No. 1 (30). P. 77–83 (in Ukrainian).
12. Zaichenko S. V., Shevchuk S. P., Harnets V. M. Tryvymirne modeliuvannia protsesu rolykovoho ushchilnennia stovburnoho kriplennia. [Three-Dimensional Modeling of Process of Roller Consolidation of Column Fastening]. *Mining, construction, road and meliorative machines.* 2012. No. 79. P. 40–45 (in Ukrainian).
13. Prykhodko Ya. S., Harnets V. M. Vzaiemouzghodzhenist roboty mekhanizmiv pry rolyko-ekstruziinomu formuvanni bahatopustotnykh vyrobiv. [Interconsistency of Operation of Mechanisms at Roller and Extrusive Formation of Multihollow Products]. *Branch mechanical engineering, construction.* 2012. No. 1 (31). P. 305–310 (in Ukrainian).
14. Loveikin V. S., Pochka K. I. Vyznachennia optymalnoho znachennia kuta zmishchennia kryvoshypiv rolykovoi formuvalnoi ustanovky z rekuperatsiinym pryvodom. [Determination of Optimum Value of a Corner of Shift of Cranks of Roller Forming Installation with the Recuperative Drive]. *Automation of productions in mechanical engineering and instrument making.* National University 'Lviv Polyequipment'. 2007. No. 41. P. 127–134 (in Ukrainian).
15. Loveikin V. S., Pochka K. I. Vyznachennia navantazhen v elementakh rolykovykh formuvalnykh ustanovok. [Definition of Loadings in Elements of Roller Forming Installations]. *Collection of scientific works of Ukrainian state academy of railway transport*. 2008. No. 88. P. 15–20 (in Ukrainian).
16. Loveikin V. S., Pochka K.I Vyznachennia navantazhen v elementakh rolykovoi formuvalnoi ustanovky. [Definition of Loadings in Elements of Roller Forming Installation]. *Theory and practice of construction.* 2007. No. 3. P. 19–23 (in Ukrainian).
17. Loveikin V. S., Pochka K. I. Doslidzhennia dynamichnykh navantazhen v elementakh rolykovykh formuvalnykh ustanovok. [Research of Dynamic Loadings in Elements of Roller Forming Installations]. *Formation of Modern Science – 2012*: Materials VIII of the intern. sci. and pract. conf. Section 18. Technical science. Formation of information technologies, (Praha, 2012). Praha, 2012. P. 20–25 (in Ukrainian).
18. Loveikin V. S., Pochka K. I. Doslidzhennia navantazhen v elementakh rolykovoi formuvalnoi ustanovky z vrivnovazhenym pryvodom. Avtomatyzatsiia vyrobn. protsesiv u mashynobud. ta pryladobud. [Research of Loadings in Elements of Roller Forming Installation with the Balanced Drive]. *Automation of productions in mechanical engineering and instrument making.* National University 'Lviv Polyequipment'. 2015. No. 49. P. 73–79 (in Ukrainian).
19. Loveykin V. S., Pochka K. I. Analiz dinamicheskogo uravnoveshivaniya privodov mashin rolikovogo formovaniya. [Analysis of Dynamic Equilibration of Drives of Machines of Roller Formation]. MOTROL. *Commission of Motorization and Energetics in Agriculture*. Lublin-Rzeszow. 2016. Vol. 18. No 3. P. 41–52 (in Russian).
20. Ustanovka dlia formuvannia vyrobiv z betonnykh sumishei [Installation for Formation of Products from Concrete Mixes]: pat. 50032 UA, IPC B28B 13/00. Publ. 25.05.2010 (in Ukrainian).
21. Loveykin V. S., Pochka K. I. Obgruntuvannya parametriv energetichno vrivnovazhenogo privodu rolikovoї formuvalnoї ustanovki. [Justification by the Parameter of Energetically Balanced Drive of Roller Forming Installation]. *Technology of construction.* 2014. No. 32. P. 25–32 (in Ukrainian).
22. Loveikin V. S., Pochka K. I. Obhruntuvannia parametriv enerhetychno vrivnovazhenoho pryvodu rolykovoi formuvalnoi ustanovky. [The Analysis of Unevenness of the Movement of Roller Forming Installation with Energetically Balanced Drive]. *Vibrations in the equipment and technologies*. 2010. No 4 (60). P. 20–29 (in Ukrainian).
23. Loveikin V. S., Kovbasa V. P.,. Pochka K. I. Dynamichnyi analiz rolykovoi formuvalnoi ustanovky z enerhetychno vrivnovazhenym pryvodom. [The Dynamic Analysis of Roller Forming Installation with Energetically Balanced Drive]. *Scientific bulletin of the National university of bioresources and environmental management of Ukraine*. Series of the technician and power engineering specialist of agro-industrial complex. 2010. Issue 144. Pt. 5. P. 338–344 (in Ukrainian).
24. Orlov I. N. (Ed.). Elektrotekhnicheskiy spravochnik. V 3 t. T. 2. Elektrotekhnicheskie izde-liya i ustroystva [Electrotechnical Reference Book. Vol. 2. Electrotechnical Products and Devices. Moscow: Jenergoatomizdat, 1986. 712 p. (in Russian).
25. Sheynblit A. Ye. Kursovoe proektirovanie detaley mashin: Course Design of Details of Machines: Manual for Technical Schools. Moscow: Vysshaja shkola, 1991. 432 p. (in Russian).
26. Degtyarev Yu. I. Metody optimizatsii. Optimization Methods. Moscow: Sov. radio, 1980. 272 p. (in Russian).
27. Rekleytis G., Reyvindran A., Regsdel K. Optimizatsiya v tekhnike. Optimization in the Equipment. In 2 books. Book 1. Translation from English. M.: Mir, 1986. 352 p. (in Russian).

Received 11 May 2018